Research Article

Hassan M. Magbool, Abdullah M. Zeyad*, Aliakbar Mahmoudi Kouch Aksaraei, and Megat Azmi Megat Johari

Effect of incorporating ultrafine palm oil fuel ash on the resistance to corrosion of steel bars embedded in high-strength green concrete

https://doi.org/10.1515/rams-2024-0072 received May 03, 2024; accepted November 08, 2024

Abstract: Durability degradation in reinforced concrete (RC) constructions is commonly attributed to the steel reinforcement corrosion caused by chloride. The utilization of supplemental cementitious resources, such as waste materials from industrial and agricultural sectors, typically improves the impermeability and strengthens concrete resistance to corrosion, sulfate, and acid attacks. Therefore, the prevention of steel reinforcement corrosion is greatly important in resolving challenges related to the durability and stability of RC structures, particularly when utilizing agriculture waste materials. This approach also serves as a solution for waste disposal. The aim of this study is to investigate the corrosionresistant characteristics of high-strength concrete that contains ultrafine palm oil fuel ash (U-POFA) as a partial replacement for cement. Four high-strength green concrete (HSGC) mixes were investigated in this study with a partial replacement of ordinary Portland cement (OPC) by U-POFA at 0, 20, 40, and 60% by mass. The aim of this study is to analyze the workability, strength activity index (SAI), compressive strength, rapid chloride permeability, linear polarization resistance (LPR) by different measurement methods, and four-probe resistivity measurement by electrical resistivity measurement method of over a curing period of 7, 28, 60, and 90 days. The use of U-POFA in the different mixes results in improved workability, SAI, compression strength, and chloride penetration resistance compared with the

zero-POFA mix. It is clear from the study results that adding U-POFA as a partial replacement for OPC improved the corrosion resistance of HSGC mixtures. Thus, the incorporation of U-POFA 60% succeeded in reducing the chloride ion penetration by 80% and the LPR by 93% at the test age of 90 days, compared to the reference mixture.

Keywords: HSC, polarization resistance, ultrafine palm oil fuel ash

1 Introduction

The expected annual expenditure for the repair and rehabilitation of reinforced concrete (RC) structures in the United States amounts to \$20 billion. Research findings indicate that approximately 40% of the total cost can be related to the corrosion of steel reinforcement [1]. The degradation of steel reinforcing bars by corrosion is a crucial factor that significantly impacts the durability of RC concrete. The corrosion of steel bars in concrete structures is prevented through the implementation of several protective measures, including the application of an anti-rust coating, the utilization of materials with low permeability and porosity, and the incorporation of chemical-resistant properties to withstand the alkaline environment of the concrete [2-4]. The durability of RC structures is significantly influenced by the external atmosphere and surrounding conditions [5–7]. The durability degradation in RC structures due to chloride-induced corrosion of steel rebar is well acknowledged as a significant factor [8-12]. The rusting of the steel reinforcing bars in structures can be categorized into two different classifications: direct corrosion, which arises from the oxidation of metal or acid exposure, and indirect corrosion, which occurs by electrochemical reaction [13]. The occurrence of corrosion in steel reinforcement reduces their cross-sectional dimensions and generates by-products that possess a greater volume relative to their initial size. Corrosion is a frequently

e-mail: azmohsen@jazanu.edu.sa

Hassan M. Magbool: Civil and Architectural Engineering Department, College of Engineering and Computer Sciences, Jazan University, Jazan, Saudi Arabia

Aliakbar Mahmoudi Kouch Aksaraei, Megat Azmi Megat Johari: School of Civil Engineering, Universiti Sains Malaysia, Engineering Campus, 14300, Nibong Tebal, Penang, Malaysia

^{*} Corresponding author: Abdullah M. Zeyad, Civil and Architectural Engineering Department, College of Engineering and Computer Sciences, Jazan University, Jazan, Saudi Arabia,

encountered problem that arises when steel reinforcement is exposed to the combined effects of water and oxygen. This chemical reaction results in the formation of iron oxide, which in turn causes volume increase. The degree of volumetric expansion in steel during the corrosion process depends on the oxidation level, leading to a maximum amplification of 6.5 times [14,15]. This phenomenon generates tensile force within the concrete structure matrix, leading to crack development and detachment between the reinforcement and the concrete [16-18]. The incidence of bar corrosion can be related to various factors, including variations in temperature, level of humidity, salinity degrees, and chemical interactions. The corrosion of steel bars is a major factor in determining the durability of buildings; thus, controlling and preventing these problems are important. Chloride penetration can be significantly impacted by the changes made to the concrete mixture compositions.

Concrete exhibits higher sustainability in terms of energy consumption and carbon emissions per unit volume than alternative construction materials, such as steel. Nevertheless, the extensive use of concrete in comparison with other construction materials has negated its sustainable advantage [19]. Portland cement (PC), the primary binder in concrete, is responsible for approximately 8–10% of the world's anthropogenic carbon emissions and consumes approximately 3% of the world's energy [20]. Therefore, developing green concrete is imperative to fulfill future concrete requirements while preserving natural resources. Green concrete refers to any type of concrete that has a lower amount of embodied energy and carbon emissions than conventional concrete [21]. Furthermore, green concrete effectively integrates various waste resources as either a binder or aggregate [22]. By-products and industrial wastes have grown to be major environmental concerns; thus, recycling them has attracted interest given the benefits of reducing building costs, avoiding adverse effects on the environment, and utilizing resources and natural energy. The concrete industry remarkably contributes to environmental sustainability by repurposing waste as building raw materials, leading to substantial positive effects on the environment [23]. In addition to sustainability concerns, the requirement for strong and durable concrete has driven the advancement of green concrete, which can withstand loads and different harmful influences on the environment [24]. Environmentally friendly concrete provides exceptional fresh and hardened properties compared with traditional concretes, thereby reducing maintenance expenses and construction timelines and providing an extended lifespan [19].

The structural characteristics of the pores and micro cracks in the hardened paste are the primary factors influencing concrete durability when exposed to external

chlorides. Important factors in the mix design remarkably affect the diffusion coefficient of concrete. These factors include the water-to-cement ratio (W/C), the maturity of the concrete after initial exposure to chloride, and the presence of supplementary cementitious materials (SCMs) [1,25]. Over a period of several decades, numerous researchers have utilized agricultural and industrial waste materials, including palm oil fuel ash (POFA) [26], waste steel slag [27], silica fume (SF) [28], and fly ash (FA) [29] in concrete. The density of the concrete is increased by substituting cement with mineral admixtures or pozzolanic materials, such as pulverized fly ash, silica fume, nano silica, and metakaolin. [30]. The SCM ingredients are commonly employed to improve the impermeability of concrete as well as its resistance to corrosion, acid attack, and sulfate assault [31], POFA is a valuable pozzolanic by-product material that is found in various regions worldwide. The POFA production process entails burning the remaining fruit bunches, palm kernel shells, and palm fibers at temperatures ranging from 800 to 1,000°C [29,32]. The amount of POFA generated in Malaysia alone rose from three million metric tons in 2007 [33] to four million metric tons in 2010 [34], and this upward trend continues to persist to the present day. Thailand's annual production of POFA amounts to approximately 100,000 tons [35]. Therefore, utilizing agricultural waste materials, such as POFA, is imperative to mitigate environmental issues linked to concrete. Prolonged accumulation of POFA waste leads to environmental contamination. The use of these resources is anticipated to enhance the environment by mitigating the disposal of wastes in open areas and landfills [36].

The utilization of POFA in the form of ultrafine particles (referred to as U-POFA) has demonstrated favorable effects on the engineering characteristics of concrete, thereby enhancing its mechanical and fluid transport features [37,38]. Furthermore, the use of POFA in the manufacture of concrete enhances the formation of high-strength concrete (HSC) as well as ultra-high-performance concrete [39]. Using the POFA in high-strength green concrete (HSGC) offers a sustainable option that comes with multiple advantages. Moreover, when manufacturing green concrete, this approach might enhance environmental sustainability by mitigating waste disposal problems and providing a cost-efficient substitute.

The experimental investigation conducted by Zeyad *et al.* [40] evaluated the incorporation of U-POFA in concrete as a means of improving its compressive strength. The researchers have shown that the incorporation of U-POFA has a crucial role in improving the workability, transport, and strength properties of HSC. The values of compressive strength reported for the HSC mixes, including 20–60% of U-POFA, were approximately 108–114 MPa. According to the study by Thomas *et al.* [41], adding POFA as a partial replacement for PC decreased chloride penetration and

permeability, increasing compressive strength. The researchers, Hamada et al. [26], conducted a series of studies examining the potential use of POFA as a sustainable alternative to PC in the production of green concrete. The conclusion drawn by the researchers is that the use of POFA with fine particles as an environmentally friendly construction material provides numerous advantages to concrete structures, specifically in terms of enhancing their strength as well as durability properties [42–46]. Alsubari et al. [47] performed the rapid chloride permeability test (RCPT). Various proportions of modified treated POFA (MT-POFA) were employed, namely, 30, 50, and 70%, as a substitute for ordinary Portland cement (OPC) in the preparation of self-compacting concrete (SCC). The results indicated that the SCC with MT-POFA exhibited significant durability against chloride and high temperatures. Moreover, the SCC using MT-POFA exhibited superior performance to the control SCC. In addition, Alani et al. [48] observed that the inclusion of polytetrafluoroethylene fiber and U-POFA produced high-performance concrete that showed remarkable resistance to chloride ion penetration within a 7-day period. The resistance was found to be significantly enhanced at 28 days of age. The structural integrity of concrete is damaged when exposed to highly acidic environments. The chemical resistance of mixes with treated palm oil fuel ash (T-POFA) was investigated by Alsubari et al. [49]. The experiment involved immersing the concrete cubes (measuring 100 mm) in a solution of hydrochloric acid with a concentration of 3%. The experimental findings demonstrate that the addition of T-POFA enhanced resistance to the effects of hydrochloric acid solutions compared with the samples without T-POFA. The influence of an attack by sulfuric acid can be more serious than that of a sulfate attack, as shown by Bassuoni and Nehdi [50]. This finding is primarily because of the dissolving impact caused by sulfate and hydrogen ions. Furthermore, the transport properties of U-POFA-incorporated HSC was evaluated by Zeyad et al. [51]. Their results suggested that adding U-POFA delayed the transport and penetration of chlorides, eventually increasing their strength properties. Similar results were obtained by Hassan et al. [52] when they examined the fluid transport properties of fiber-reinforced green concrete incorporating U-POFA.

Therefore, steel reinforcement corrosion must be presented to resolve challenges related to the durability and stability of RC structures, particularly when utilizing agriculture waste materials, which can also serve as a solution for waste disposal. Nevertheless, to the best of the authors' knowledge, no research has examined the corrosion resistance of HSGC with the inclusion of U-POFA, especially by assessing the polarization resistance and resistivity of the concrete mixes. Therefore, this study primarily aims to perform these experiments to assess how the inclusion of U-POFA affects the corrosion resistant performance of HSGC. The linear polarization resistance (LPR) test was used to measure the corrosion rate on the steel bars. Four HSGC mixes with a partial replacement U-POFA of 0, 20, 40, and 60% for OPC by mass were investigated. The effects of including U-POFA in HSGC mixes on various properties, including workability, compressive strength, chloride permeability, polarization resistance, and resistivity were examined. The investigation was conducted at curing durations of 7, 28, 60. and 90 days.

The significance of the work lies in the observation that incorporating reasonable amounts of cement substitutes, such as U-POFA, reduced further the low permeability and porosity, thereby improving resistance against corrosion of steel bars. This aspect must be considered and thoroughly investigated because this characteristic may have the potential to significantly enhance the corrosion resistance of steel bar in HSGC that contains substantial amounts of U-POFA. In addition, U-POFA exhibits environmental sustainability by mitigating waste disposal problems and providing a cost-efficient substitute.

2 Experimental study

The flowchart of the experimental program is shown in Figure 1. The experimental program was conducted in two phases. The first phase was for the U-POFA production process, whereas the second phase was for the casting and testing of specimens.

2.1 Materials

The concrete mixes used were fabricated employing OPC, granite coarse aggregate, river sand fine aggregate, U-POFA, and superplasticizer (SP).

2.1.1 Portland cement

ASTM Type 1 (OPC) was used in accordance with the specifications provided by ASTM C150 [53]. The PC was produced by Cement Industries of Malaysia Berhad. The specific gravity (SG) of the cement was 3.15. In addition, Table 1 displays the chemical specifications of cement.

2.1.2 POFA

The approach employed in this investigation followed the methods of Johari et al. [39] for the preparation of the U-POFA. The initial collection of the original palm oil fuel ash

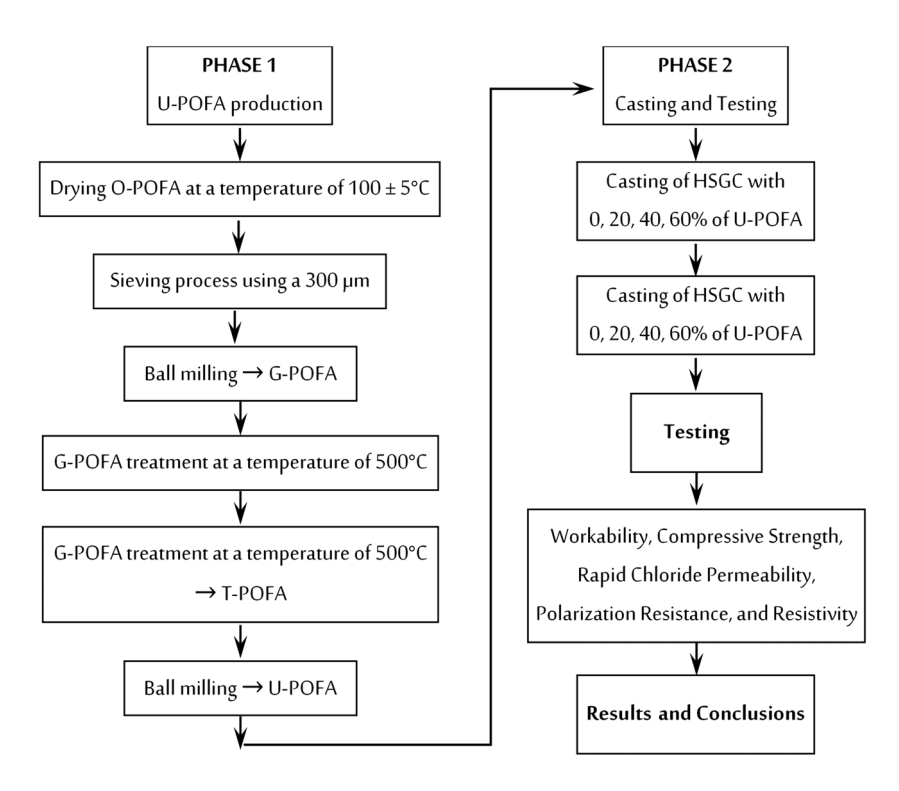


Figure 1: Flowchart of the experimental program.

(O-POFA) was conducted at a palm oil mill located in Nibong Tebal, Malaysia. Subsequently, the O-POFA samples were subjected to a drying process in an electric oven set at a temperature of $100 \pm 5^{\circ}$ C for a duration of 24 h. This drying procedure was implemented to eliminate any existing moisture content within the samples. Subsequently, the dried O-POFA underwent sieving using a 300 µm sieve to exclude particles of larger size. Then, the O-POFA was subjected to grinding using ball milling equipment, thereby forming the ground POFA (G-POFA). The G-POFA was subsequently subjected to thermal treatment in a gas furnace set at a temperature of 500°C for a duration of 90 min. This process aimed to diminish the presence of unburnt carbon and obtain treated POFA (T-POFA) [54]. Thereafter, the T-POFA underwent additional grinding within the same ball milling equipment to produce the U-POFA. The control of consistency in the U-POFA generated was achieved through the implementation of various measures. These measures included the precise determination of the quantity of POFA introduced into the ball milling equipment, the regulation

of milling speed and time, the management of the POFA layer thickness during heating, the control of heating duration, and the adjustment of heating temperature. Figure 2 illustrates the generation procedures of the U-POFA. Table 2 presents the observed alterations in the particle size of the POFAs during every phase. Figure 3 depicts the distribution of particle sizes of the POFAs during different treatment phases. The U-POFA had a median particle size of 2.21 µm, which was the smallest among the samples analyzed. After analyzing the median particle sizes of OPC and O-POFA, the U-POFA exhibited a decrease in size of 78.29 and 86.73%. U-POFA performs better in HSC because it can produce a higher paste volume and has a lower SG than G-POFA. The high amount of unburned carbon in G-POFA restricts its consistency, prevents the micro-filling effect, and lowers the rate at which it hydrates and facilitates pozzolanic reactions. Therefore, in this study, U-POFA was used. Furthermore, Figure 4 displays the scanning electron microscope (SEM) images, illustrating the variations in particle size among the various phases of POFA.

Table 1: Chemical specifications of PC, G-POFA, and U-POFA

Item	SiO ₂	Al ₂ O ₃	Fe ₂ O ₃	CaO	MgO	P ₂ O ₅	K ₂ O	SO ₃	TiO ₂	MnO	Na ₂ O	С	LOI
PC	18.81	4.54	3.2	65.77	0.78	0.08	1.18	3.54	0.20	0.19	0.09	_	2.52
G-POFA	45.37	5.09	3.76	3.87	3.22	2.99	4.11	0.23	0.19	0.06	0.07	30.60	26.80
U-POFA	62.08	7.09	5.92	5.39	4.24	3.84	5.57	0.23	0.27	0.09	0.10	4.74	3.45

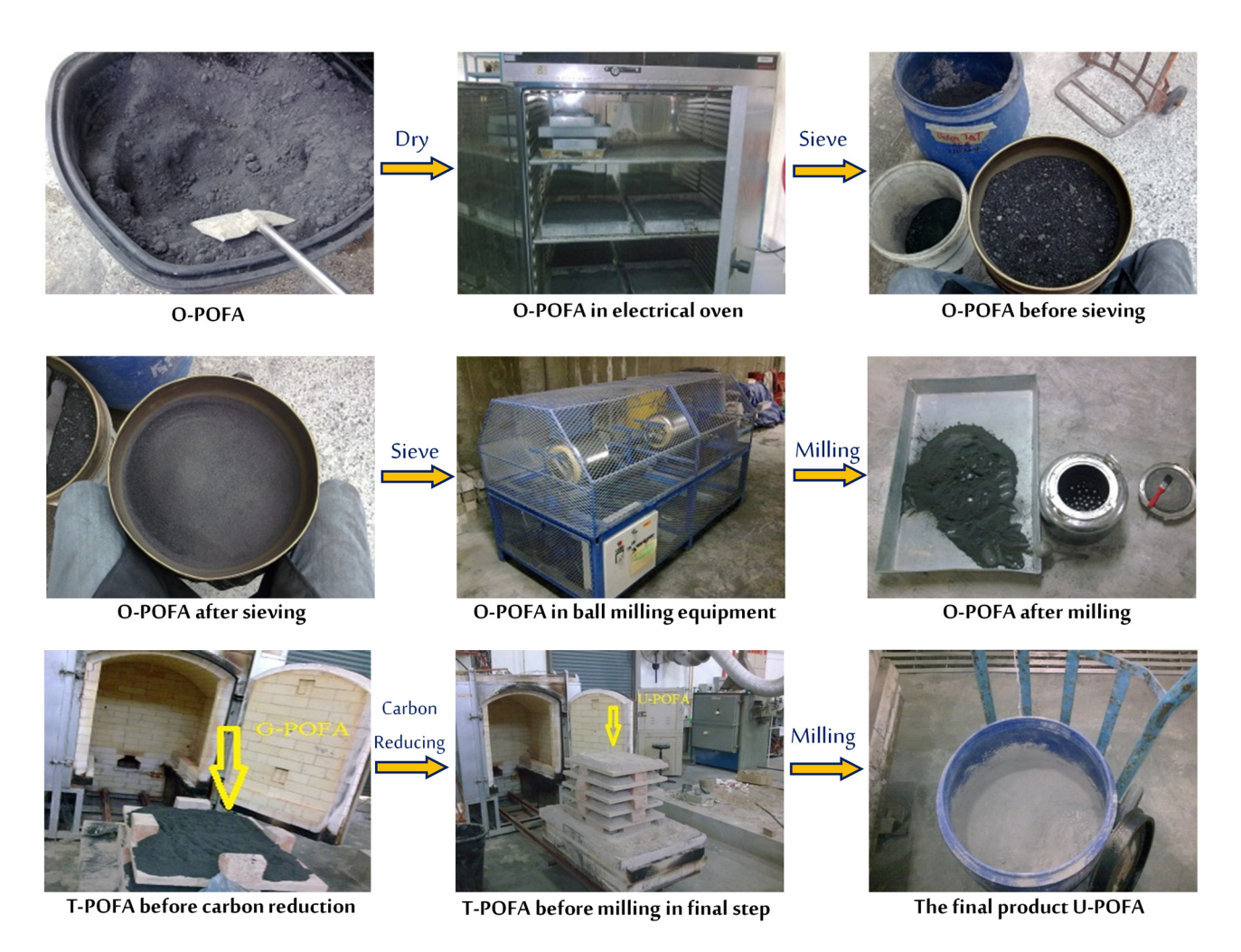


Figure 2: Production procedures of the U-POFA.

DE GRUYTER

Figure 4 illustrates a significant reduction in the size of the POFA particles at different stages of the treatment process, consistent with the numerical results shown in Table 2. Table 1 displays the chemical compositions of PC, G-POFA, and U-POFA as determined using X-ray fluorescence (XRF) analysis. The results suggest that the treatment method led to a notable enhancement in the G-POFA's chemical composition, with a substantial reduction in the amount of carbon by 85.4%. Furthermore, a significant decrease of

Table 2: Median particle size of POFAs and PC

Materials	Median particle size (μm)	Surface area (cm²⋅g ⁻¹)
PC	10.18	320
O-POFA	16.66	210
G-POFA	12.35	480
U-POFA	2.21	1,550

87.12% was observed in the level of the LOI content on comparing G-POFA with U-POFA.

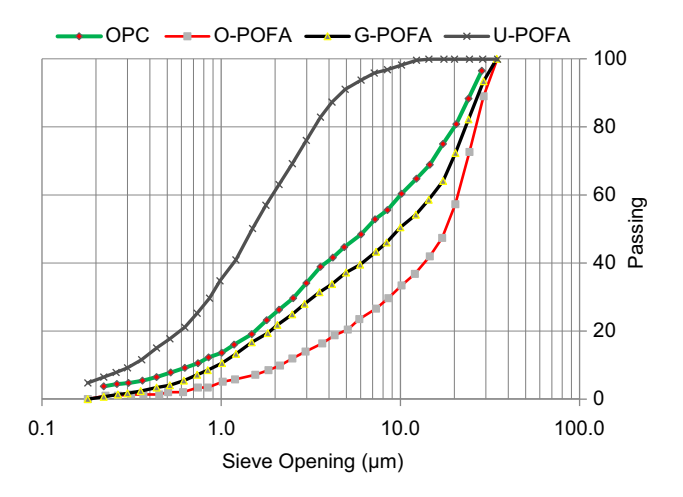


Figure 3: Particle size distribution of POFAs and PC.

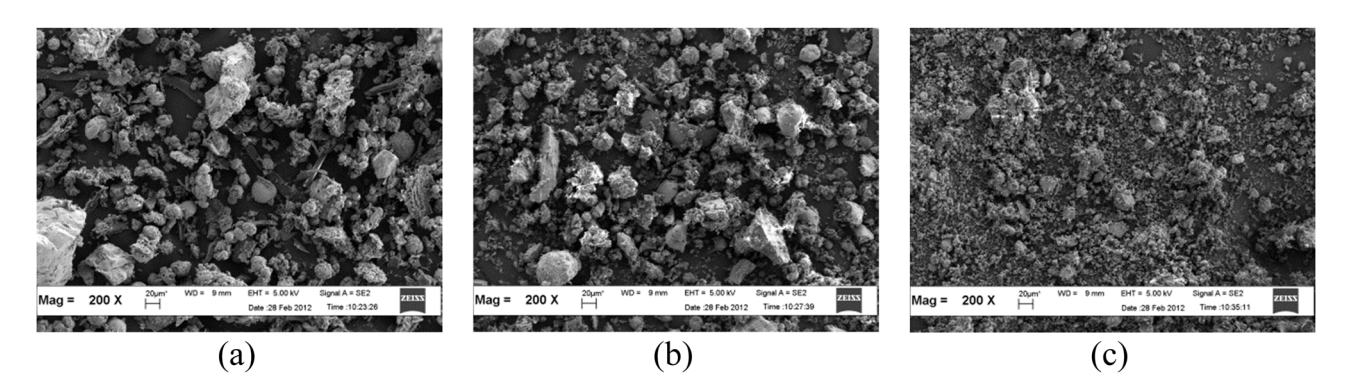


Figure 4: SEM images of POFAs. (a) O-POFA. (b) G-POFA. (c) U-POFA.

2.1.3 Aggregate

Natural river sand was utilized in the study. The aggregate had a SG value of 2.75, a fineness modulus of 3.10, and a water absorption rate of 0.61%, satisfying the requirements outlined in ASTM C128 [55] and ASTM C136 [56]. The coarse aggregates include crushed granite, possessing a max size of 12.5 mm. The bulk density of these aggregates was 1,550 kg·m⁻³, calculated using ASTM C29 [57]. According to ASTM C127 [58], the coarse aggregates exhibited a SG of 2.70 and a water absorption rate of 0.49%. A sieve analysis was carried out on the coarse and fine aggregates to obtain the gradation curves in accordance with the standards outlined in ASTM C33 [59]. These curves are illustrated in Figure 5.

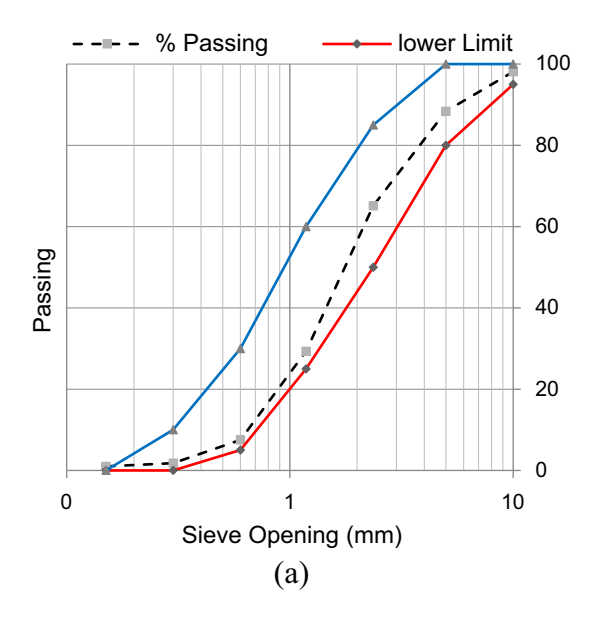
2.1.4 Steel reinforcement bars (rebar)

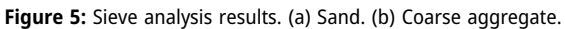
A typical rebar with a diameter of 10 mm was employed to perform corrosion experiments, representing the circumstances

encountered by steel reinforcement placed in an HSGC sample. A preliminary cleaning of the steel rods is essential to attain accurate results. The cleaning process was executed as follows: the steel rods were subjected to an initial brushing operation with an electrical brush that was fitted with a wide-wired head. Subsequently, to remove any oil or other impurities, the rods were subjected to a cleaning procedure utilizing acetone, followed by a meticulous drying process using a towel.

2.1.5 Chemical admixture

A chemical admixture, known as GLENIUM ACE 393 SP, manufactured by BASF Chemical Company was applied to decrease the water-to-cement ratio and enhance the workability of the HSGC mixes. According to the specifications of the manufacturer, the product is classified as a high-range water reducer and is referred to as Type F according to the standards outlined in ASTM C494 [60].





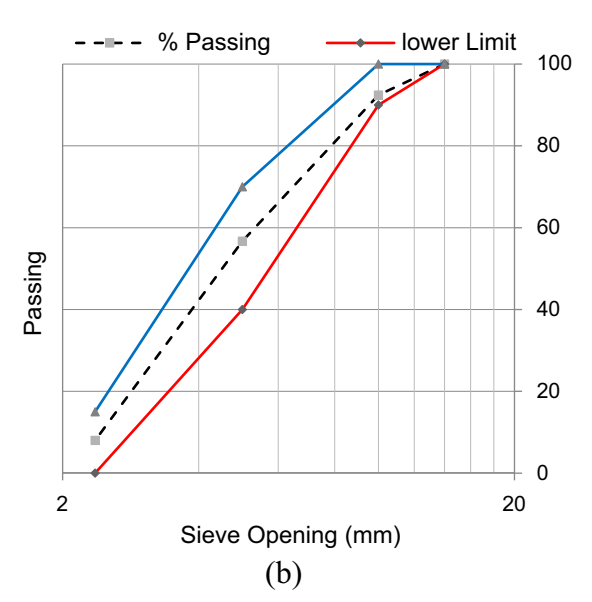


Table 3: HSGC mix proportions in kg·m⁻³

Proportions	Mixes					
	ОРС	20UP	40UP	60UP		
Water	154	154	154	154		
PC	550	440	330	220		
U-POFA	_	110	220	330		
Coarse aggregate	933	933	933	933		
Sand	842	842	842	842		
SPr	12.1	12.1	12.1	12.1		

2.2 Mixture proportion

A minimum initial target strength of 80 MPa at 28 days was established for the HSGC specimens in all groups, while maintaining a water-binder ratio of 0.28. Four concrete mixes were created using the amounts stated in Table 3. The initial mixture served as the control, consisting of 100% OPC. In the subsequent mixtures, the OPC was substituted with different proportions of U-POFA. Three different substitution ratios of U-POFA were utilized, namely, 20% (referred to as 20UP), 40% (referred to as 40UP), and 60% (referred to as 60UP), as illustrated in Table 3. The mixing process began by adding the prescribed amounts of sand and coarse aggregates to the mixer. Thereafter, the PC or binder was incorporated to aid comprehensive mixing. The duration of this particular stage spans from 3 to 4 min when the aggregates and binder are meticulously blended to attain a uniform dry mixture. Then, the water and the SP were incorporated into the mix, and the mixing process was maintained for a period that ranged from 4 to 6 min.

2.3 Specimen preparation

The specimens were cast in three layers into the respective steel molds, wherein each layer underwent compaction through the use of a vibrating table. This process was employed to eradicate the presence of air bubbles and attain a homogeneous mixture. Figure 6(a) depicts the vibration phase during the concrete casting operation. The specimens subsequent to the casting process are illustrated in Figure 6(b). The molds remained undisturbed for a specific period, and then they were enveloped with a moist canvas and left for a period of 24 h to harden. The next day, the samples were removed from the molds and then submerged in a water tank for curing. Subsequently, the specimens were prepared for the corresponding tests. The specimens were subjected to different curing times of 7, 28, 60, and 90 days.

2.4 Test methods

The tests were conducted within a specific period (7, 28, 60, and 90 days) to avoid the effects of changes in laboratory conditions, thereby influencing the accuracy of the results. The tests were also conducted under saturated surface dryness for all specimens and under the same laboratory conditions as recommended by Piro et al. [61].

2.4.1 Strength activity index (SAI)

ASTM C 109 specifications are followed in the preparation of pozzolanic strength activity index specimens. To partially replace pozzolanic materials by 20% of the cement mass used in the strength test of cement mortar for SAI tests, ASTM C311 specifications are followed. The mixture proportions are shown in Table 4.

2.4.2 Compressive strength

The compressive strength test was conducted on concrete cubes with dimensions of 100 mm. The experimental setup



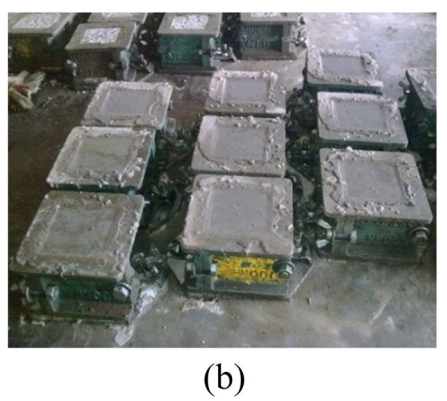


Figure 6: HSGC specimen's preparation. (a) Compaction of specimens in a vibrating table. (b) Specimens after casting.

Table 4: Proportion of cement mortar mixtures for SAI

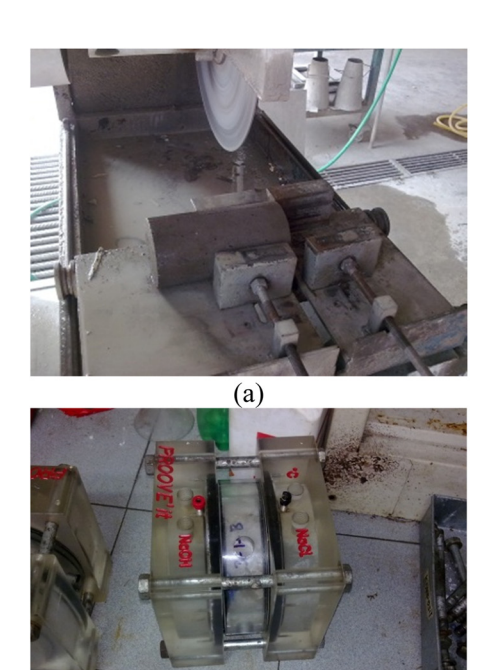
Mix code	OPC	POFA	FA	Water
		(k	g·m ^{−3})	
ОРС	550	0	1,549	242.5
O-POFA	440	110	1,530	
G-POFA	440	110	1,530	
U-POFA	440	110	1,530	

involved the utilization of a compression machine, specifically the ADR-Auto type, which had a capacity of 3,000 kN. According to the provisions in BS EN [62], the tests were conducted at three different curing ages: 7, 28, and 90 days. The results for each mix are obtained by taking the average of the three cube results.

2.4.3 RCPT

RCPT was conducted on the specimens according to ASTM C1202 [63] to measure the concrete conductance. Prior to testing, the specimens were created by sectioning cylindrical concrete with a diameter of 100 mm and a height of 200 mm into slices. The specimens consisted of cylindrical concrete slices of 100 mm in diameter with a thickness of 50 ± 2 mm. The specimens underwent testing at the ages of

7, 28, and 90 days. The procedure for cutting the sliced specimens is shown in Figure 7(a). In this experiment, the slices were initially placed within a vacuum saturation tank (Figure 7(b)), where they were subjected to a pressure of approximately 133 Pa or 1 mm Hg for a duration of 3 h. Subsequently, the concrete slices were immersed in water within the tank for approximately 1 h while undergoing the vacuum procedure. The final stage in the preparation of the concrete slices for testing involved the cessation of vacuum pumping and the subsequent release of pressure. The specimens remained immersed in the water tank for a duration of up to 18 h. During the experimental procedure. individual slices of concrete were positioned within a cell situated between two reservoirs. The positive reservoir contained approximately 200 ml of a 0.30 N sodium hydroxide (NaOH) solution, while the negative reservoir contained approximately 200 ml of a 3.0% sodium chloride (NaCl) solution. This arrangement is visually depicted in Figure 7(c). Following the installation of the samples and instruments, as depicted in Figure 7(d), a continuous direct current of 60 V was applied to the samples for a duration of 6 h. The total charge passed was individually determined and recorded at 5 min intervals for each specimen. The given results represent the average of two specimens within each group. Theoretically, a higher penetration of chloride charge would result in greater conductivity and an increase in current within the samples.



(c)

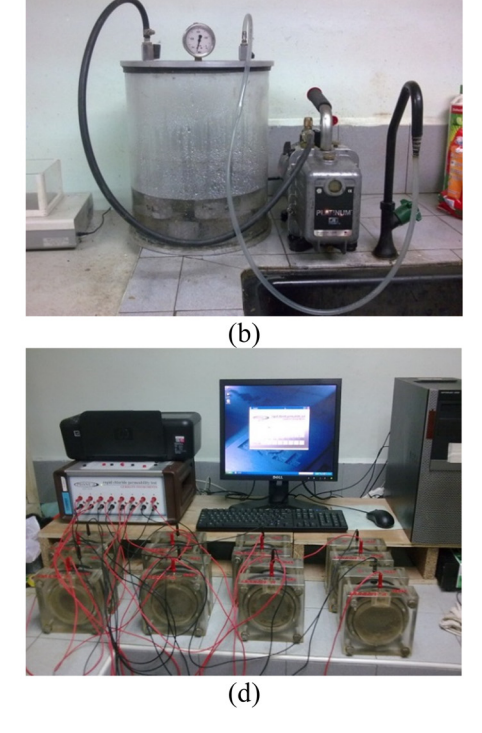


Figure 7: RCPT procedures: (a) Samples preparation; (b) vacuum saturation tank; (c) test cell; and (d) test setup.

2.4.4 LPR test

The LPR test is a technique to monitor the corrosion rate. It was performed in this study for this purpose at 7, 28, 60, and 90 days based on ASTM G59 [64]. The schematic setup of the test is depicted in Figure 8(a). The Autolab PGSTAT302N instrument (Figure 8(b)) equipped with Metrohm Nova 1.7 software was employed to determine the LPR and corrosion rates of the specimens. The samples were placed in a cell container filled with the 3.5% NaCl solution to obtain accurate results. The cell configuration comprised three distinct electrodes: stainless steel acting as the counter electrode (CE), the concrete samples serving as the working electrodes (WE), and a Metrohm Ag/AgCl standard electrode functioning as the reference electrode (RE), as visually depicted in Figure 8(c). The polarization test was conducted using the Metrohm Nova 1.7 program. The test parameters included a step potential of 0.001 V and a scan rate of 0.05 V·s⁻¹. In addition, for the steel bars inserted in the specimens, an equivalent weight of 27.925 g·mol⁻¹ and density of 7.86 g·cm⁻³ were set. Furthermore, the current range of a working electrode is 1 mA and its start/end potential is 0.25 V. Moreover, the surface area of the working electrode was set to 14.13 cm². The samples were subjected to LPR tests according to the specified setup

settings, and the subsequent results were observed and recorded. Subsequently, the Tafel linear extrapolation method was utilized, followed by the application of the Tafel slope analysis tool. Furthermore, the polarization resistances and the corrosion rates of the specimens were measured.

2.4.5 Resistivity measurement

A four-probe resistivity meter (RESI) depicted in Figure 9(a) was utilized for verification of the electrical resistivity of the concrete samples. The resistivity measurements were obtained from five different locations: the right corner, the left corner, the middle right, the middle left, and the center (Figure 9(b)). The resistivity measurement presented for each sample was determined by calculating the average of three readings. In the middle of each sample, a steel bar was embedded to assess its effect on the resistivity of the sample. The test was performed at 7, 28, 60, and 90 days. The given results are the average values obtained from three different tested samples for all mixes after the curing process. The findings have been computed and graphed for analysis so that they can be understood. The findings based on the research of Mehta and Monteiro [65] are compared in Table 5.

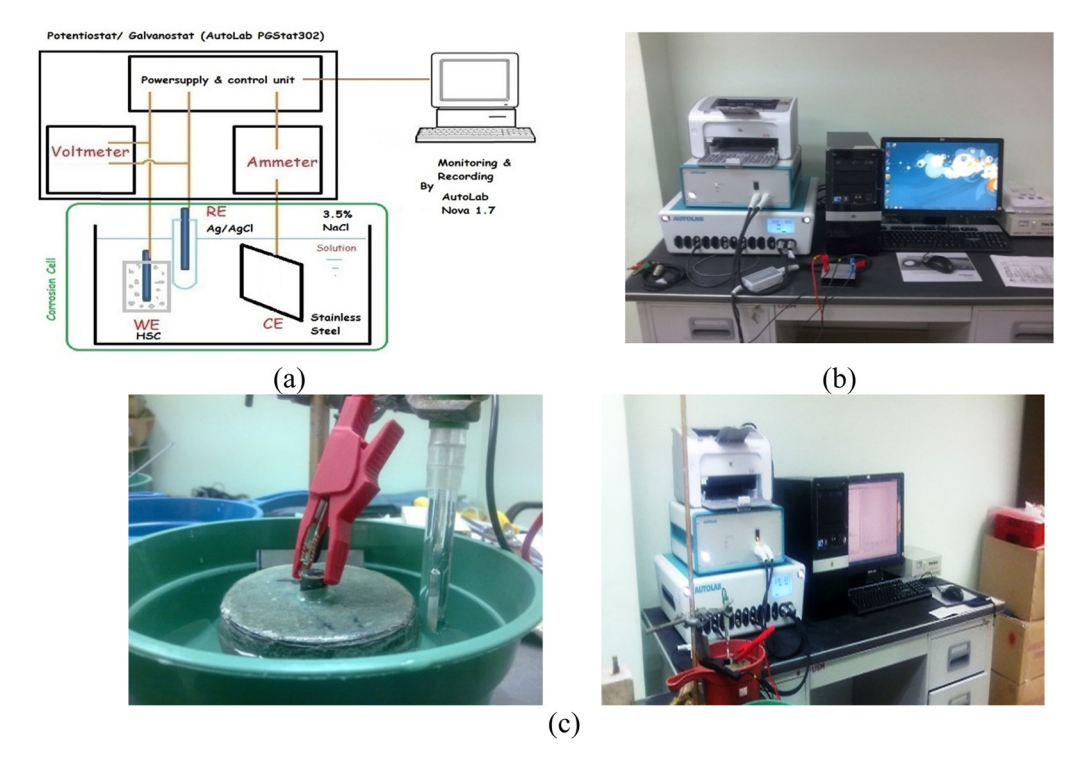
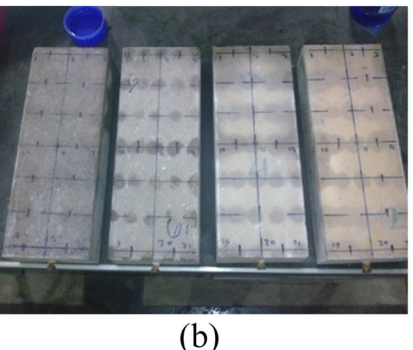


Figure 8: LPR procedures: (a) schematic setup; (b) Autolab PGSTAT302N cell; and (c) test cell with HSGC specimen.





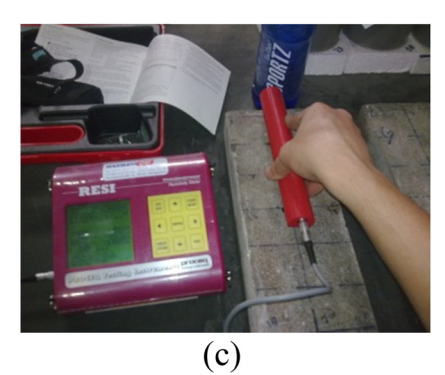


Figure 9: RESI procedures: (a) RESI instrument; (b) sample preparation; and (c) resistivity measurement.

3 Results and discussion

3.1 Slump test results

Table 6 shows the slump values for all the HSGC mixes conducted based on ASTM C143 [66]. The table displays data that demonstrate an increase in slump value for HSGC mixes 20UP, 40UP, and 60UP, compared with the control mix. The slump value increased by 25 mm for the 20UP mix, 40 mm for the 40UP mix, and 45 mm for the 60UP mix, which represented an increase of 13.5, 18.9, and 21.6% for the 20UP, 40UP, and 60UP mixes, respectively, compared with the OPC mix. Nevertheless, a slight reduction in the increase rate was observed compared with a smaller level of U-POFA replacement, as observed in a previous study [39]. Johari et al. [39] demonstrated that the observed phenomenon can be attributed to the U-POFA's lower SG and greater surface area than cement. U-POFA particles are usually finer than OPC particles. These smaller particles can occupy the empty spaces between the coarser cement particles,

Table 5: Resistivity interpretation [65]

Likely corrosion rate	Negligible	Low	High	Very high
Concrete resistivity (kΩ·cm)	>20	10-20	5–10	<5

Table 6: Slump test of HSGC mixes

Materials	Slump test (mm)
OPC	185
O-POFA	210
G-POFA	220
U-POFA	225

resulting in a more compact arrangement and increasing the internal friction resistance within the mixture. Moreover, the spherical morphology of U-POFA particles, contrary to the angular shape of OPC grains, can enhance the smoothness of the texture and improve the lubricating effect [29]. The U-POFA utilization in the HSGC mix increased the quantity of the binder paste volume compared with the HSGC mix without U-POFA. Consequently, the decreased U-POFA's particle size, compared with OPC, could potentially result in improved workability. Therefore, a higher quantity of U-POFA must be used to decrease the dosage of SP or the W/C, depending on the desired slump value.

3.2 SAI results

SAI test was performed for all cement mortar mixes at the testing ages of 7 and 28 days. The SAI results are shown in Table 7. First, the results show that both G-POFA and U-POFA mixes meet the ASTM C618 standard specification, which requires a compressive strength of at least 75% of the reference mix at the age of 7 and 28 days. At the test ages of 7 and 28 days, the U-POFA mixture showed an increase in compressive strength of more than 100% compared to the reference mixture. The findings reveal that the milling process (G-POFA) enhanced the strength index results, surpassing those of O-POFA mixes. In addition, the heat

Table 7: SAI results (%)

Test age (days)	7	28
OPC	100	100
O-POFA	68	72
G-POFA	86	98
U-POFA	119	128

treatment and subsequent milling (U-POFA) achieved the best results compared to other mixtures. In the case of G-POFA, the efficiency of the reaction of very fine particles in a short time, compared to the larger particle size, may account for the increase in compressive strength. The role of removing the remaining carbon in increasing the material's efficiency also contributes to the increase in pressure of the heat-treated fine particles, as in the U-POFA mixture [40].

3.3 Compressive strength results

Figure 10 shows the compressive strength results for all the HSGC mixes. The data in Figure 10 demonstrate that the addition of high levels of U-POFA (*i.e.*, 40 and 60%) had a notable adverse effect on the compressive strength of all HSGC specimens, particularly at 7 days. The compressive

strengths of the 40UP and 60UP mixes after 7 days were 70.63 and 60.1 MPa, respectively, whereas the OPC mix recorded a strength of 76.0 MPa. Several researchers have found similar findings [51,67,68]. This degradation could be attributed to the reduction in PC content by partial substitution with U-POFA. Nevertheless, as the curing period was extended, the HSGC specimens with U-POFA exhibited a strength higher than that of the OPC specimen. This finding can be attributed to the occurrence of a pozzolanic reaction involving the U-POFA and calcium hydroxide (CH). After 90 days, the results showed that the compressive strength of the HSGC demonstrates enhancements when U-POFA is employed as a substitute for PC at levels of 20, 40, and 60%. This finding implies that the inclusion of U-POFA in a significant quantity has a beneficial effect on the compressive strength of HSGC mixes. In this regard, the incorporation of up to 60% U-POFA by weight of cement possesses the capability to enhance the compressive strength of the HSGC to a similar

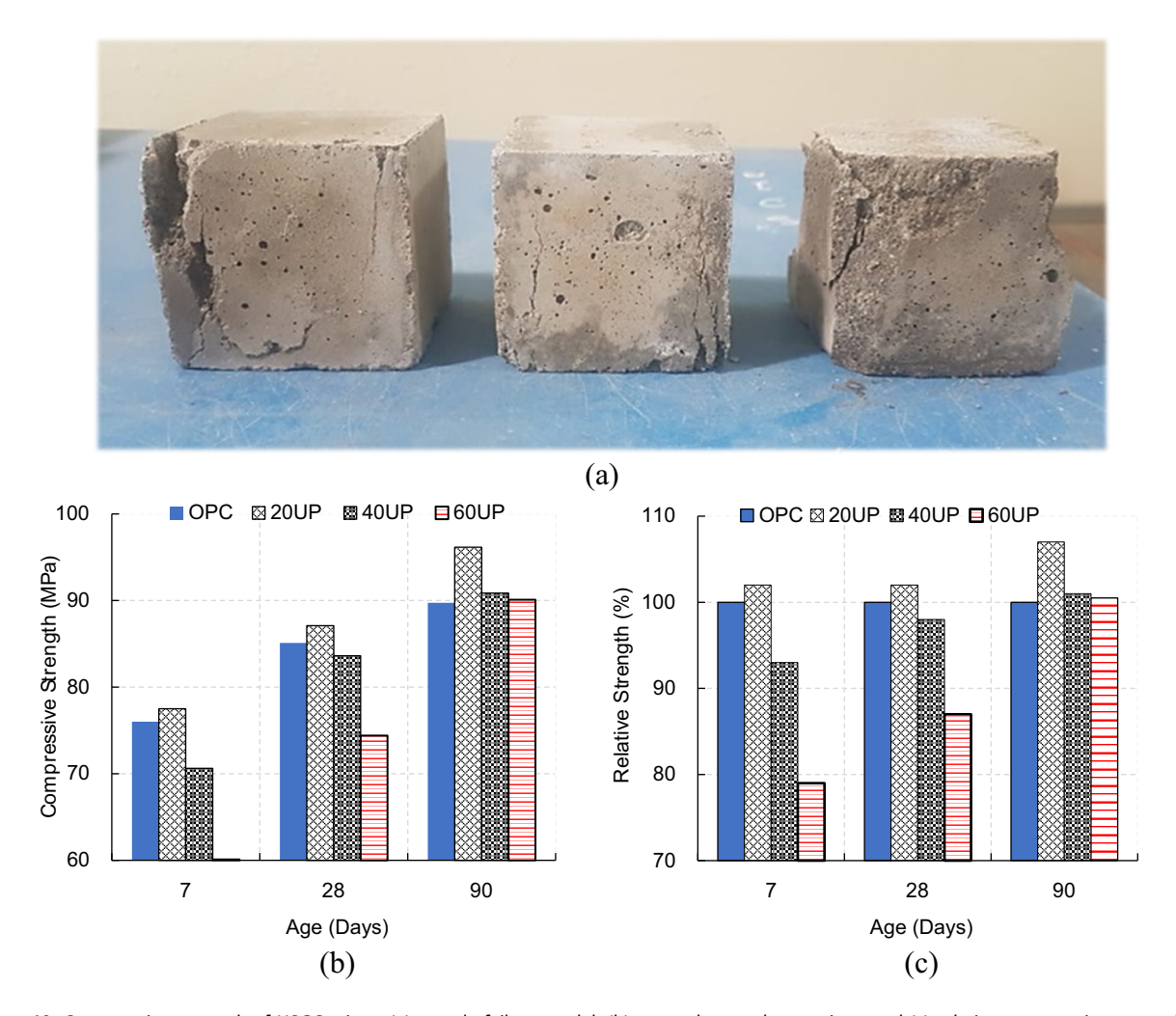


Figure 10: Compressive strength of HSGC mixes: (a) sample failure model; (b) strength growth over time; and (c) relative compressive strength.

degree to concrete mix comprising 100% PC, at 90 days of curing period, as illustrated in Figure 10. The compressive strength was the highest when 20% U-POFA was used (20UP mix) compared with all other HSGC mixes after 7 and 28 days of curing, as shown in Figure 10. However, the increase in strength is only slightly greater than that of the concrete mix comprising 100% cement. Nevertheless, after a period of 90 days of curing, a significant gain in strength was observed, as depicted in Figure 10. Although the compressive strength decreased at the early ages of curing (i.e., 7 and 28 days) as the substitution level of PC increased to 40%, a slight increase in compressive strength was observed after 90 days compared with the OPC. The strength of the HSGC exhibited a greater reduction upon the addition of 60% U-POFA. This reduction was especially noticeable throughout the 7- and 28-days curing periods, surpassing the observed decreases in all other mixes. Nevertheless, the compressive strength exhibits a progressive enhancement throughout the curing period (i.e., from 7–28 days). However, over a curing duration of 90 days, the 60UP mix had a compressive strength (89.6 MPa) that was similar to that of the OPC mix (89.7 MPa), as demonstrated in Figure 10. The results show that adding 20% U-POFA did not reduce the compressive strength during the 7, 28, and 90-day curing duration. This approach markedly enhanced the level of compressive strength. Therefore, in cases where compressive strength at the early ages must be improved, the most suitable amount of U-POFA substitution must be determined and applied. The current study demonstrates that a substitution ratio of 20% is appropriate. Several previous studies have reported similar findings, including the studies conducted by several authors [35,39,51,69]. Jaturapitakkul *et al.* [70] reported the impact of the fineness and filler of G-POFA on the improvement of compressive strength. Hence, to attain this purpose, a minimum of two pivotal factors must be analyzed. First, the incorporation of SCMs with improved pozzolanic properties can enhance the production of additional calcium silicate hydrate gel in the cement paste matrix. This feature offers notable benefits in relation to the improvement of concrete strength. This specific potentiality emerges within the HSGC that integrates different SCMs. Second, the particle size of pozzolan remarkably affects the improvement of the microstructure of the concrete matrix, resulting in the formation of a denser microstructure.

3.4 RCPT

The assessment of chloride ion penetration into concrete is reliant on the evaluation of chloride permeability, which is

determined by measuring the total charge passing (TCP) through concrete samples. The findings of the RCPT in this investigation are presented in Table 8. The table shows that the TCP of all HSGC specimens decreased considerably with the integration of the U-POFA. For instance, at 7 days, the decreased percentages compared with the OPC sample reached 12.0, 35.4, and 58.4% for 20UP, 40UP, and 60UP, respectively. At 28 days, the TCP results showed significant decreases in values for 20UP, 40UP, and 60UP, reaching 63.9, 80.6, and 82.3%, respectively, when compared with the OPC sample. After 90 days of curing, the TCP values decreased significantly for the 20UP, 40UP, and 60UP samples, reaching 60.9, 76.2, and 80.7%, respectively, compared with the OPC sample. From a broad perspective, the findings illustrate two key observations. A clear correlation exists between the age of samples and the penetration rate of chloride ions. As the samples age, the penetration rate of chloride ions consistently decreases. Nevertheless, the rates exhibit a significant decrease in samples containing U-POFA and demonstrate a positive relationship with the increasing dosage of U-POFA replacement in the HSGC samples. The second observation is the reduction in chloride ion permeation when the U-POFA substitution rate is increased compared with the OPC at the same age. Consequently, the chloride permeability of the HSGC incorporating the U-POFA is reduced compared with the specimens composed entirely of OPC. In addition, the results of this study agree with those of earlier studies that considered the resistance of concrete mixes to chloride ion penetration that contained up to 40% G-POFA and other pozzolanic materials, such as rice husk ash and fly ash [71,72]. Nevertheless, the preceding findings indicate a diminished positive impact as a result of the substantial presence of unburned carbon. In addition, the findings of this investigation are consistent with the results reported by Johari et al. [39], providing further confirmation of this study. An important factor to be considered is the highly reactive nature of U-POFA as a pozzolanic material, which has the ability to decrease the permeability of concrete to water and gas. This outcome is achieved by

Table 8: RCPT results

Days		TCP (C)					
	ОРС	20UP	40UP	60UP			
7	4,147 —	3,649 -12.0%	2,677 -35.4%	1,727 -58.4%			
28	2,073	749 -63.9%	403 -80.6%	366 -82.3%			
90	961 —	375 -60.9%	229 -76.2%	185 -80.7%			

Table 9: Polarization resistance by the LPR method

Days		P	_R (Ω)	
	ОРС	20UP	40UP	60UP
7	863	1,532	2,144	2,751
28	838	3,207	4,879	7,057
60	862	3,317	5,769	9,305
90	1,007	4,477	8,772	16,457

promoting the formation of a denser microstructure and reducing the overall porosity. One possible explanation is that the presence of an additional calcium silicate hydrate gel, resulting from the interaction of U-POFA with water and CH during the hydration process, can fill the capillary pores. The presence of admixtures with pozzolanic properties may hinder the early age growth of strength at high replacement levels due to the dilution effect. However, as the concrete ages, the increasing amount of calcium silicate hydrate gel might contribute to improved strength. This condition can also lead to the refinement of pores within the concrete, thereby enhancing its resistance to the permeation of chloride ion. Therefore, the incorporation of a significant proportion of U-POFA as a replacement to PC for cement can potentially improve the durability of concrete structures [32,39,73].

3.5 LPR test

Table 9 presents the polarization resistance ($P_{\rm R}$) ascertained by the LPR test. At 7 days, the polarization resistances of the OPC, 20UP, 40UP, and 60UP samples were 863, 1,532, 2,144, and 2,751 Ω , respectively. As the U-POFA replacement dosage increased, the polarization resistance increased. However, the polarization resistance of the OPC sample experienced a slight decrease to 838 Ω at 28 days. The $P_{\rm R}$ of the OPC sample increased by almost 15% after 90 days, whereas the $P_{\rm R}$ of the 20UP, 40UP, and 60UP samples increased by 65.9, 75.6, and 83.3%, respectively. Evidently,

Table 10: C_R by the LPR method

Days	C _R ×10 ⁻⁴ (mm·year ⁻¹)				
	ОРС	20UP	40UP	60UP	
7	89	43	34	25	
28	90	25	15	10	
60	88	22	13	7	
90	73	17	9	5	

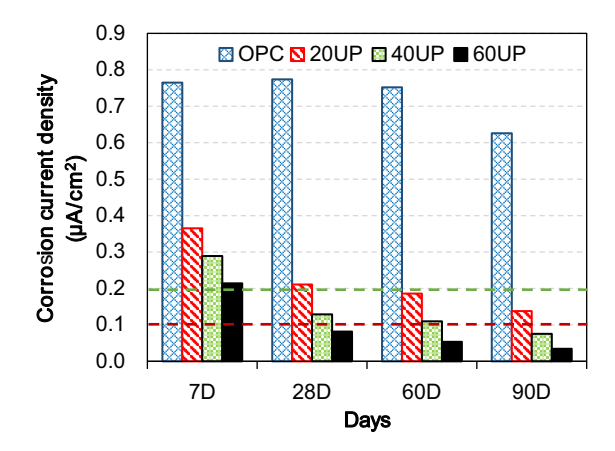


Figure 11: Limitations of corrosion current density.

the U-POFA enhanced the $P_{\rm R}$ of the HSGCs by 4.44 to 16.3 times compared with that of the OPC at 90 days.

Table 10 presents the corrosion rates (C_R) of the tested specimens at 7, 28, 60, and 90 days using the LPR method. At 7 days, the C_R of 20UP, 40UP, and 60UP decreased by approximately 51.7, 61.8, and 71.9%, respectively, compared with the OPC corrosion rate. A similar pattern was observed after 28 days, where the C_R of 20UP, 40UP, and 60UP reduced by approximately 72.2, 83.3, and 88.9%, respectively. In addition, the C_R of the three HSGC mixes with U-POFA decreased from 75 to 92.0% at 60 days, whereas the reductions in the C_R varied from 76.7 to 93.2% at 90 days, as shown in Table 10. The experimental findings demonstrate that incorporating U-POFA as SCMs with strong pozzolanic properties notably decreases the C_R of steel reinforcement within HSGC specimens. This reduction is directly related to the amount of U-POFA used as a substitute.

Furthermore, numerous investigations demonstrated that a corrosion current density ranging from 0.1-0.2 μ A·cm⁻² is an indicator of a passive state for steel within concrete. This passive state implies the absence of corrosion or, at most, minimal corrosion occurrences [74]. Figure 11 illustrates the corrosion current density, which was calculated using the LPR approach for all the samples analyzed in this study. The corrosion current density must be limited within the range delineated by the green lines. The maximum limit is indicated by the green line at 0.2 μA·cm⁻², whereas the lower limit is represented by the yellow line at 0.1 μA·cm⁻². Nevertheless, a decrease in the corrosion current density indicates an improvement in corrosion resistance. The findings indicate that after 28 days of curing and beyond, all U-POFA mixes exhibit a minimal corrosion level, indicating that the U-POFA mixes are in a passive state. By contrast, the OPC samples exhibit a corrosion current density that is four to five times greater after 28 days of curing and beyond, as shown in Figure 11. This finding indicates that, throughout

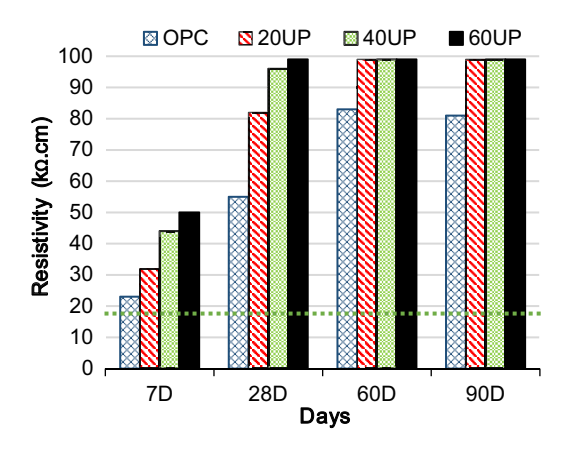


Figure 12: Resistivity of samples at different ages.

this period, all OPC samples are subject to a moderate level of corrosion risk. However, the RCPT results showed a strong positive relationship with the $C_{\rm R}$ and corrosion current densities obtained from the LRP test. Therefore, the results of this investigation suggest that the incorporation of a significant quantity of U-POFA as a partial replacement material for cement in HSGC mixes may effectively mitigate the $C_{\rm R}$ and corrosion current density.

3.6 Four-probe resistivity measurement

Figure 12 shows the mean electrical resistivity measurements of OPC, 20UP, 40UP, and 60UP samples at 7, 28, 60, and 90 days. The results show that the resistivity of the samples was proportional to the curing age as well as the replacement levels of the U-POFA. This phenomenon may be ascribed to the pozzolanic reaction process, in which the pozzolanic activity increases with time, refining the pores inside the concrete and inducing higher resistivity. At 7 days, the 20UP, 40UP, and 60UP samples demonstrated a resistivity of 55, 83, and 81 kΩ·cm, respectively, whereas the OPC sample only achieved 23 kΩ·cm. The 40UP and 60UP samples reached the highest range of resistivity (99 $k\Omega$ -cm) at the age of 28 days, whereas the 20UP sample required 90 days to reach this resistivity. However, the OPC sample had a starting resistivity of only 23 kΩ·cm at 7 days and arrived at 50 k Ω ·cm after 90 days. Therefore, the incorporation of the U-POFA dramatically increased the electrical resistivity of the HSGC samples to the highest available measurement that the resistivity apparatus can record (99 k Ω ·cm). The research conducted by Ramezanianpour et al. [75] reveals that no significant correlation exists between the compressive strength and concrete resistivity. This lack of association can be attributed to the distinct mechanisms behind the two properties. Consequently,

employing resistivity as a reliable indicator for assessing compressive strength is not recommended. Furthermore, the findings of this study for each age group, when compared with the research conducted by Mehta and Monteiro [65], showed resistivity values >20 k Ω ·cm. This finding indicated a low probability of corrosion for a steel bar that is embedded within concrete. However, Newman and Choo [76] indicated that the probability of corrosion of all samples is negligible because the resistivity values depicted in Figure 12, represented by the green dotted line, surpass the threshold of 20 k Ω ·cm.

The experimental findings reveal discrepancies between reality and testing. In the experimental test, limited time and laboratory settings are considered. The environmental circumstances or extended exposure times might affect the concrete performance. Although variations exist, the experimental results offer crucial insights into the main stages involved in comprehending the behavior of U-POFA on corrosion resistance of steel bars embedded in HSGC. This study offered an additional understanding of the process of bar corrosion using U-POFA up to 60% and a curing period of up to 90 days. Generally, U-POFA incorporation has succeeded in enhancing the long-term durability of concrete structures, especially under harsh environmental exposures. This approach is also a cost-effective and environmentally friendly waste disposal solution.

4 Conclusions

The experimental findings provide the following conclusions:

- 1) The U-POFA inclusion improves the workability of the concrete mixes. the slump experienced a respective increase of 13.5, 18.9, and 21.6% for the 20UP, 40UP, and 60UPC mixes, respectively, compared with the OPC mix. Therefore, a higher quantity of U-POFA must be used to reduce the dosage of SP or the W/B ratio, depending on the desired slump value.
- 2) The HSGC mix with 20% of U-POFA exhibited an increase of up to 8% in compressive strength over all ages. For U-POFA inclusion at levels 40% and 60%, the compressive strength decreased at 7 and 28 days, respectively. Nevertheless, the utilization of such levels demonstrated comparable longterm compressive strength compared with the OPC mix.
- 3) The use of U-POFA in HSGC specimens significantly reduced chloride permeability. For example, in the 60UP mix, the reduction ratios reached 58.4, 82.3, and 80.7% at 7, 28, and 90 days, respectively, indicating its potential to improve the durability and sustainability of concrete constructions.

- 4) The addition of the U-POFA dramatically increased the electrical resistivity of the HSGC samples. The U-POFA enhanced the polarization resistance of the HSGCs by 4.44–16.3 times compared with that of the OPC at 90 days. The findings indicated a low probability of corrosion of the steel bar that is embedded within concrete.
- 5) Using U-POFA as partial replacement for OPC greatly improved the corrosion resistance of HSGC mixtures. Thus, compared to the reference mixture, the addition of 60% U-POFA succeeded in lowering the chloride ion penetration by 80% at the test age of 90 days, where the U-POFA 60% reduced the linear polarization resistance by 93% from the reference mixture.
- 6) The UPOFA incorporation dramatically increased the electrical resistivity of the HSGC samples to the highest available measurement that the resistivity apparatus can record.

Generally, the use of U-POFA at 60% of the PC content is highly recommended because of the environmental benefits and cost-effectiveness of U-POFA as a green pozzolanic material. This approach also enhances the corrosion resistance of HSGC, thereby improving the concrete structures' durability, especially in harsh environments. However, further investigation is required, particularly for the following aspects: assessing the long-term durability under cyclic loading conditions or resistance to different corrosive substances may be of utmost importance, especially when using greater volume of U-POFA. The long-term improvement of the HSGC mixtures that include U-POFA should be performed to evaluate persistent corrosion resistance and durability enhancements.

Acknowledgments: The authors extend their appreciation to the Deputyship for Research and Innovation, Ministry of Education in Saudi Arabia for funding this research work through the project number ISP23-131.

Funding information: This research was funded by the Deputyship for Research and Innovation, Ministry of Education in Saudi Arabia through the project number ISP23-131.

Author contributions: All authors have accepted responsibility for the entire content of this manuscript and approved its submission.

Conflict of interest: The authors state no conflict of interest.

Data availability statement: All data generated or analyzed during this study are included in this published article.

References

- [1] Holland, B., P. Alapati, K. E. Kurtis, and L. Kahn. Effect of different concrete materials on the corrosion of the embedded reinforcing steel. *Corrosion of steel in concrete structures*, Woodhead Publishing, Sawston, Cambridge, 2023, pp. 199–218.
- [2] Faroz, S. A., N. N. Pujari, and S. Ghosh. Reliability of a corroded RC beam based on Bayesian updating of the corrosion model. *Engineering Structures*, Vol. 126, 2016, pp. 457–468.
- [3] Lee, H.-S., H. G. Kim, J.-S. Ryou, Y. Kim, and B.-H. Woo. Corrosion state assessment of the rebar: Experimental investigation by ambient temperature and relative humidity. *Construction and Building Materials*, Vol. 408, 2023, id. 133598.
- [4] Murthy, A. R., P. K. Prasanna, G. Nipun, K. Srinivasu, K. Gandla, A. H. Khan, et al. Analysing the influence of ground granulated blast furnace slag and steel fibre on RC beams flexural behaviour. Scientific Reports, Vol. 14, No. 1, 2024, id. 4914.
- [5] Bertolini, L., B. Elsener, P. Pedeferri, E. Redaelli, and R. B. Polder. Corrosion of steel in concrete: prevention, diagnosis, repair, John Wiley & Sons, Hoboken, New Jersey, U.S., 2013.
- [6] Pilvar, A., A. A. Ramezanianpour, H. Rajaie, and S. M. M. Karein. Practical evaluation of rapid tests for assessing the chloride resistance of concretes containing silica fume. *Computers and Concrete, An International Journal*, Vol. 18, No. 4, 2016, pp. 793–806.
- [7] Poursaee, A. and U. M. Angst. Principles of corrosion of steel in concrete structures. In *Corrosion of steel in concrete structures*, Elsevier, Amsterdam, Netherlands, 2023, pp. 17–34.
- [8] Bensabra, H., A. Franczak, O. Aaboubi, N. Azzouz, and J.-P. Chopart. Inhibitive effect of molybdate ions on the electrochemical behavior of steel rebar in simulated concrete pore solution. *Metallurgical and Materials Transactions A*, Vol. 48, 2017, pp. 412–424.
- [9] Broomfield, J. P. Corrosion of steel in concrete: understanding, investigation and repair, Crc Press, United States, Boca Raton, Florida, 2023.
- [10] Gomes, C., Z. Mir, R. Sampaio, A. Bastos, J. Tedim, F. Maia, et al. Use of ZnAl-layered double hydroxide (LDH) to extend the service life of reinforced concrete. *Materials*, Vol. 13, No. 7, 2020, id. 1769.
- [11] Wu, M. and J. Shi. Beneficial and detrimental impacts of molybdate on corrosion resistance of steels in alkaline concrete pore solution with high chloride contamination. *Corrosion Science*, Vol. 183, 2021, id. 109326.
- [12] Yu, B., J. Liu, and B. Li. Improved numerical model for steel reinforcement corrosion in concrete considering influences of temperature and relative humidity. *Construction and Building Materials*, Vol. 142, 2017, pp. 175–186.
- [13] Sakr, K. Effect of cement type on the corrosion of reinforcing steel bars exposed to acidic media using electrochemical techniques. *Cement and Concrete Research*, Vol. 35, No. 9, 2005, pp. 1820–1826.

- [14] Bhargava, K., A. K. Ghosh, Y. Mori, and S. Ramanujam. Model for cover cracking due to rebar corrosion in RC structures. *Engineering Structures*, Vol. 28, No. 8, 2006, pp. 1093–1109.
- [15] Liang, Y. and L. Wang. Prediction of corrosion-induced cracking of concrete cover: A critical review for thick-walled cylinder models. *Ocean Engineering*, Vol. 213, 2020, id. 107688.
- [16] Li, C.-Q., J. J. Zheng, W. Lawanwisut, and R. E. Melchers. Concrete delamination caused by steel reinforcement corrosion. *Journal of Materials in Civil Engineering*, Vol. 19, No. 7, 2007, pp. 591–600.
- [17] Montemor, M. F., A. M. P. Simoes, and M. G. S. Ferreira. Chloride-induced corrosion on reinforcing steel: from the fundamentals to the monitoring techniques. *Cement and concrete composites*, Vol. 25, No. 4–5, 2003, pp. 491–502.
- [18] Poupard, O., V. L'Hostis, S. Catinaud, and I. Petre-Lazar. Corrosion damage diagnosis of a reinforced concrete beam after 40 years natural exposure in marine environment. *Cement and Concrete Research*, Vol. 36, No. 3, 2006, pp. 504–520.
- [19] Sivakrishna, A., A. Adesina, P. Awoyera, and K. R. Kumar. Green concrete: A review of recent developments. *Materials Today: Proceedings*, Vol. 27, 2020, pp. 54–58.
- [20] Jaf, D. K. I., P. I. Abdulrahman, A. S. Mohammed, R. Kurda, S. M. Qaidi, and P. G. Asteris. Machine learning techniques and multiscale models to evaluate the impact of silicon dioxide (SiO₂) and calcium oxide (CaO) in fly ash on the compressive strength of green concrete. *Construction and Building Materials*, Vol. 400, 2023, id. 132604
- [21] Garg, R., R. Garg, N. O. Eddy, M. A. Khan, A. H. Khan, T. Alomayri, et al. Mechanical strength and durability analysis of mortars prepared with fly ash and nano-metakaolin. *Case Studies in Construction Materials*, Vol. 18, 2023, id. e01796.
- [22] Zeyad, A. M., M. A. Johari, Y. R. Alharbi, A. A. Abadel, Y. M. Amran, B. A. Tayeh, et al. Influence of steam curing regimes on the properties of ultrafine POFA-based high-strength green concrete. *Journal of Building Engineering*, Vol. 38, 2021, id. 102204.
- [23] Piro, N. S., A. S. Mohammed, and S. M. Hamad. The impact of GGBS and ferrous on the flow of electrical current and compressive strength of concrete. *Construction and Building Materials*, Vol. 349, 2022, id. 128639.
- [24] Hamada, H., F. Abed, A. Alattar, F. Yahaya, B. Tayeh, and Y. I. Aisheh. Influence of palm oil fuel ash on the high strength and ultra-high performance concrete: A comprehensive review. *Engineering Science and Technology, an International Journal*, Vol. 45, 2023, id. 101492.
- [25] Jagadesh, P., A. Ramachandramurthy, P. Rajasulochana, M. A. Hasan, R. Murugesan, A. H. Khan, et al. Effect of processed sugarcane bagasse ash on compressive strength of blended mortar and assessments using statistical modelling. *Case Studies in Construction Materials*, Vol. 19, 2023, id. e02435.
- [26] Hamada, H. M., G. A. Jokhio, F. M. Yahaya, A. M. Humada, and Y. Gul. The present state of the use of palm oil fuel ash (POFA) in concrete. *Construction and Building Materials*, Vol. 175, 2018, pp. 26–40.
- [27] Piro, N. S., A. Mohammed, S. M. Hamad, and R. Kurda. Electrical resistivity-compressive strength predictions for normal strength concrete with waste steel slag as a coarse aggregate replacement using various analytical models. *Construction and Building Materials*, Vol. 327, 2022, id. 127008.
- [28] Burhan, L., K. Ghafor, and A. Mohammed. Modeling the effect of silica fume on the compressive, tensile strengths and durability of

- NSC and HSC in various strength ranges. *Journal of Building Pathology and Rehabilitation*, Vol. 4, 2019, pp. 1–19.
- [29] Zeyad, A., M. A. M. Johari, B. A. Tayeh, and I. M. Alshaikh. Influence of palm oil fuel ash on properties of high-strength green concrete. *Scientific Journal of King Faisal University (Basic and Applied Sciences)*, Vol. 20, 2019, pp. 63–72.
- [30] Emad, W., A. S. Mohammed, A. Bras, P. G. Asteris, R. Kurda, Z. Muhammed, et al. Metamodel techniques to estimate the compressive strength of UHPFRC using various mix proportions and a high range of curing temperatures. *Construction and Building Materials*, Vol. 349, 2022, id. 128737.
- [31] Al-Akhras, N. M. Durability of metakaolin concrete to sulfate attack. Cement and Concrete Research, Vol. 36, No. 9, 2006, pp. 1727–1734.
- [32] Zeyad, A. M., M. A. M. Johari, A. Abadel, A. Abutaleb, M. J. A. Mijarsh, and A. Almalki. Transport properties of palm oil fuel ash-based high-performance green concrete subjected to steam curing regimes. *Case Studies in Construction Materials*, Vol. 16, 2022, id. e01077.
- [33] Ranjbar, N., M. Mehrali, A. Behnia, U. J. Alengaram, and M. Z. Jumaat. Compressive strength and microstructural analysis of fly ash/palm oil fuel ash based geopolymer mortar. *Materials & Design*, Vol. 59, 2014, pp. 532–539.
- [34] Mujah, D. Compressive strength and chloride resistance of grout containing ground palm oil fuel ash. *Journal of Cleaner Production*, Vol. 112, 2016, pp. 712–722.
- [35] Chindaprasirt, P., S. Homwuttiwong, and C. Jaturapitakkul. Strength and water permeability of concrete containing palm oil fuel ash and rice husk–bark ash. *Construction and Building Materials*, Vol. 21, No. 7, 2007, pp. 1492–1499.
- [36] Hamada, H. M., F. Abed, S. Beddu, A. Humada, and A. Majdi. Effect of volcanic ash and natural pozzolana on mechanical properties of sustainable cement concrete: A comprehensive review. Case Studies in Construction Materials, Vol. 19, 2023, id. e02425.
- [37] Karim, R., M. F. M. Zain, M. Jamil, and N. Islam. Strength of concrete as influenced by palm oil fuel ash. *Australian Journal of Basic and Applied Sciences*, Vol. 5, No. 5, 2011, pp. 990–997.
- [38] Hamada, H., A. Alattar, B. Tayeh, F. Yahaya, and A. Adesina. Sustainable application of coal bottom ash as fine aggregates in concrete: A comprehensive review. *Case Studies in Construction Materials*, Vol. 16, 2022, id. e01109.
- [39] Johari, M. A. M., A. M. Zeyad, N. M. Bunnori, and K. S. Ariffin. Engineering and transport properties of high-strength green concrete containing high volume of ultrafine palm oil fuel ash. Construction and Building Materials, Vol. 30, 2012, pp. 281–288.
- [40] Zeyad, A. M., M. A. M. Johari, B. A. Tayeh, and M. O. Yusuf. Efficiency of treated and untreated palm oil fuel ash as a supplementary binder on engineering and fluid transport properties of highstrength concrete. *Construction and Building Materials*, Vol. 125, 2016, pp. 1066–1079.
- [41] Thomas, N., S. Mathew, K. M. Nair, K. O'Dowd, P. Forouzandeh, A. Goswami, et al. 2D MoS₂: structure, mechanisms, and photocatalytic applications. *Materials Today Sustainability*, Vol. 13, 2021, id. 100073.
- [42] Hamada, H., B. Tayeh, F. Yahaya, K. Muthusamy, and A. Al-Attar. Effects of nano-palm oil fuel ash and nano-eggshell powder on concrete. *Construction and Building Materials*, Vol. 261, 2020, id. 119790.
- [43] Hamada, H. M., A. Al-Attar, J. Shi, F. Yahaya, M. S. Al Jawahery, and S. T. Yousif. Optimization of sustainable concrete characteristics incorporating palm oil clinker and nano-palm oil fuel ash using

- response surface methodology. Powder Technology, Vol. 413, 2023, id. 118054.
- [44] Hamada, H. M., A. Alya'a, F. M. Yahaya, K. Muthusamy, B. A. Tayeh, and A. M. Humada. Effect of high-volume ultrafine palm oil fuel ash on the engineering and transport properties of concrete. Case Studies in Construction Materials, Vol. 12, 2020, id. e00318.
- [45] Hamada, H. M., G. A. Jokhio, F. M. Yahaya, and A. M. Humada. Properties of fresh and hardened sustainable concrete due to the use of palm oil fuel ash as cement replacement, Vol. 342, IOP Publishing, Bristol, England, 2018, 012035.
- [46] Hamada, H. M., G. A. Jokhio, F. M. Yahaya, and A. M. Humada. Applications of nano palm oil fuel ash and nano fly ash in concrete, Vol. 342, IOP Publishing, Bristol, England, 2018, 012068.
- [47] Alsubari, B., P. Shafigh, Z. Ibrahim, M. F. Alnahhal, and M. Z. Jumaat. Properties of eco-friendly self-compacting concrete containing modified treated palm oil fuel ash. Construction and Building Materials, Vol. 158, 2018, pp. 742-754.
- [48] Alani, A. H., N. M. Bunnori, A. T. Noaman, and T. A. Majid. Durability performance of a novel ultra-high-performance PET green concrete (UHPPGC). Construction and Building Materials, Vol. 209, 2019, pp. 395-405.
- [49] Alsubari, B., P. Shafigh, and M. Z. Jumaat. Development of selfconsolidating high strength concrete incorporating treated palm oil fuel ash. Materials, Vol. 8, No. 5, 2015, pp. 2154-2173.
- [50] Bassuoni, M. T. and M. L. Nehdi. Resistance of self-consolidating concrete to sulfuric acid attack with consecutive pH reduction. Cement and Concrete Research, Vol. 37, No. 7, 2007, pp. 1070-1084.
- [51] Zeyad, A. M., M. A. M. Johari, B. A. Tayeh, and M. O. Yusuf. Pozzolanic reactivity of ultrafine palm oil fuel ash waste on strength and durability performances of high strength concrete. Journal of Cleaner Production, Vol. 144, 2017, pp. 511-522.
- [52] Hassan, M. H., S. H. Abo Sabah, N. M. Bunnori, and M. A. Megat Johari. Fluid transport properties of normal concrete substrate and a new green fiber reinforced concrete overlay composite. Structural Concrete, Vol. 20, No. 5, 2019, pp. 1771-1780.
- [53] ASTM-C150. Standard test method for Portland cement, ed: ASTM International, West Conshohocken, PA, United States, 2016.
- [54] Chandara, C., E. Sakai, K. A. M. Azizli, Z. A. Ahmad, and S. F. S. Hashim. The effect of unburned carbon in palm oil fuel ash on fluidity of cement pastes containing superplasticizer. Construction and Building Materials, Vol. 24, No. 9, 2010, pp. 1590-1593.
- [55] ASTM-C128. Standard test method for relative density (specific gravity) and absorption of fine aggregate, ed: ASTM International, West Conshohocken, PA, United States, 2015.
- [56] ASTM-C136. Standard test method for sieve analysis of fine and coarse aggregates, ed: ASTM International, West Conshohocken, PA, United States, 2006.
- [57] ASTM-C29. Standard test method for bulk density ("unit weight") and voids in aggregate, ed: ASTM International, West Conshohocken, PA, United States, 2009.
- [58] ASTM-C127. Standard test method for relative density (specific gravity) and absorption of coarse aggregate, ed: ASTM International, West Conshohocken, PA, United States, 2015.
- [59] ASTM-C33/C33M. Standard specification for concrete aggregates, ASTM International, West Conshohocken, PA, USA, 2018.
- [60] ASTM-C496. Standard test method for splitting tensile strength of cylindrical concrete specimens, ASTM International, West Conshohocken, PA, USA, 2011.

- [61] Piro, N. S., A. S. Mohammed, and S. M. Hamad. Electrical resistivity measurement, piezoresistivity behavior and compressive strength of concrete: A comprehensive review. Materials Today Communications, Vol. 36, 2023, id. 106573.
- [62] B. EN. 12390-3, Testing hardened concrete-part 3: compressive strength of test specimens. British Standards Institution, London, United Kingdom, 2002.
- [63] ASTM-C1202. Standard test method for electrical indication of concrete's ability to resist chloride ion penetration, ed: ASTM International, West Conshohocken, PA, United States, 2019.
- [64] ASTM-G59-97. Standard test method for conducting potentiodynamic polarization resistance measurements, ed: ASTM International, West Conshohocken, PA, United States, 2014.
- [65] Mehta, P. K. and P. I. M. Monteiro, Concrete: microstructure, properties, and materials, McGraw-Hill Education, New York City, New York, U.S., 2014.
- [66] ASTM-C143/C143M. Standard test method for slump of hydrauliccement concreTE, ed: ASTM International, West Conshohocken, PA, United States, 2012.
- [67] Hassan, W. N. F. W., M. A. Ismail, H. S. Lee, M. W. Hussin, and M. Ismail. Engineering properties of high strength blended concrete enhanced with Nano POFA, 2006, Vol. 495, 1st ed., IOP Publishing, Bristol, England, 2019, 012105.
- [68] Ranjbar, N., A. Behnia, B. Alsubari, P. M. Birgani, and M. Z. Jumaat. Durability and mechanical properties of self-compacting concrete incorporating palm oil fuel ash. Journal of Cleaner Production, Vol. 112, 2016, pp. 723-730.
- Abdullah, K., M. W. Hussin, F. Zakaria, R. Muhamad, and Z. Abdul [69] Hamid. A potential partial cement replacement material in aerated concrete, Proceedings of the 6th Asia-Pacific Structural Engineering and Construction Conference (APSEC 2006), 5-6 September 2006, Kuala Lumpur, Malaysia, 2006.
- Jaturapitakkul, C., K. Kiattikomol, W. Tangchirapat, and T. Saeting. Evaluation of the sulfate resistance of concrete containing palm oil fuel ash. Construction and Building Materials, Vol. 21, No. 7, 2007, pp. 1399-1405.
- [71] Chindaprasirt, P., C. Chotetanorm, and S. Rukzon. Use of palm oil fuel ash to improve chloride and corrosion resistance of highstrength and high-workability concrete. Journal of Materials in Civil Engineering, Vol. 23, No. 4, 2011, pp. 499-503.
- [72] Chindaprasirt, P. and S. Rukzon. Strength, porosity and corrosion resistance of ternary blend Portland cement, rice husk ash and fly ash mortar. Construction and Building Materials, Vol. 22, No. 8, 2008, pp. 1601-1606.
- [73] Kroehong, W., T. Sinsiri, and C. Jaturapitakkul. Effect of palm oil fuel ash fineness on packing effect and pozzolanic reaction of blended cement paste. Procedia Engineering, Vol. 14, 2011, pp. 361-369.
- [74] ACI-222R-01. Protection of Metals in Concrete Against Corrosion. ACI 222R-01, Reported by ACI Committee, American Concrete Institute, Farmington Hills, MI, USA, Vol. 222, 2007.
- Ramezanianpour, A. A., A. Pilvar, M. Mahdikhani, and F. Moodi. [75] Practical evaluation of relationship between concrete resistivity, water penetration, rapid chloride penetration and compressive strength. Construction and Building Materials, Vol. 25, No. 5, 2011, pp. 2472-2479.
- [76] Newman, J. and B. S. Choo. Advanced concrete technology 3: processes, Elsevier, Amsterdam, Netherlands, 2003.